$^6\vec{\text{Li}}+^{12}\text{C}$ inelastic scattering at 30 and 50 MeV

P. L. Kerr, K. W. Kemper, P. V. Green, K. Mohajeri, E. G. Myers, and B. G. Schmidt
Department of Physics, Florida State University, Tallahassee, Florida 32306-3016

V. Hnizdo
Department of Physics, University of Witwatersrand, Johannesburg, 2050 South Africa
(Received 1 April 1996)

A complete set of analyzing powers (AP's), iT_{11}, T_{20}, T_{21}, and T_{22}, for 50 MeV $^{12}\text{C}(^6\vec{\text{Li}},^6\text{Li})$ elastic scattering and inelastic scattering to the $^{12}\text{C}(2^+$, 4.44 MeV), $^{12}\text{C}(0^+$, 7.65 MeV), and $^{12}\text{C}(3^-$, 9.64 MeV) states over the center-of-mass (c.m.) angular range $10°-115°$ is reported. In addition, cross sections for the excited states 3^+(2.18 MeV), 2^+(4.31 MeV), and 1^+(5.65 MeV) of ^{6}Li were measured by using the inverse-kinematics reaction $^6\text{Li}(^{12}\text{C},^{12}\text{C})$ at 100 MeV. A combined analysis of the new 50 MeV data and previous 30 MeV data has been carried out using the coupled-channels (CC) code FRESCO. Comparison of FRESCO calculations with those using the CC code CHUCK are presented. The CC calculations use an optical potential with double-folded (DF) real central, Woods-Saxon imaginary central, and Thomas real spin-orbit (SO) potentials. Calculations include reorientation terms and coupling to the first three excited states of ^{6}Li and the first two nonzerospin states of ^{12}C. The ^{6}Li coupling strengths were fixed by the measured ^{6}Li excited-state cross sections. The elastic-scattering cross sections and A.P.'s are described well. The need for an explicit SO potential is apparent in the elastic and inelastic-scattering AP's iT_{11}, more so at 30 MeV than at 50 MeV. The rank-2 AP's up to 50° c.m. arise mainly from ground-state reorientation effects. The DF potential normalization constant N approaches unity for the 50 MeV data. At both energies, the $^{12}\text{C}(2^+)$ cross sections are underestimated at large angles, and the description of the $^{12}\text{C}(3^-)$ cross sections is poor in detail. The $^{12}\text{C}(3^-)$ AP's and the $^{12}\text{C}(2^+)$ iT_{11} are not reproduced at either energy. [S0556-2813(96)05609-9]

PACS number(s): 24.70.+s, 24.10.Ht, 25.70.Bc

I. INTRODUCTION

The unexpectedly large vector analyzing powers (AP's) observed originally in polarized ^{6}Li ($^6\vec{\text{Li}}$) elastic scattering from ^{12}C and other targets [1] have since been found in $^6\vec{\text{Li}}$ scattering over a wide range of energies by these and other nuclei: ^{58}Ni [2–4], ^{26}Mg [5,6], ^{12}C [7–10], ^{9}Be [11], ^{4}He [12,13], and ^{120}Sn [14].

The large spin-dependent effects observed in these experiments were originally attributed to an explicit, or static, (folded) spin-orbit (SO) potential [2]. However, the magnitudes of the AP's for the heavier targets, e.g., ^{58}Ni, were not matched using such a SO potential, while a coupled-channels (CC) approach without an explicit SO interaction [15–18] reproduced many of the experimental data. Both the dynamic SO interaction, which arises from channel coupling, and the explicit SO potential may be present in the ^{6}Li-nucleus interaction, but the extent to which these two mechanisms of spin-orbit interaction compete with each other at the $^6\vec{\text{Li}}$ energies studied thus far is not known.

It has been suggested that the dynamic, channel-coupling-generated SO interaction dominates the explicit SO potential at energies near the Coulomb barrier, but that the two become comparable [19] at energies well above the barrier. Sakuragi has predicted that the explicit SO potential should dominate the dynamic SO interaction [20] at intermediate energies ($>$ 100 MeV/nucleon). However, it is not clear at what energy the two types of SO interaction will begin to compete.

With the development of more sophisticated polarized Li ion sources, rank-2 AP's became available, and were also found to have large values, especially the AP T_{21} [5,9]. As with the SO interaction, the role of the static versus dynamic tensor interaction in producing tensor AP's, as well as of the projectile-energy and target-mass dependence of the tensor interactions, has been a subject of considerable discussion [4,6,14,16,19,21]. In addition, it has been suggested that, in the double-folded nuclear potential formalism, the normalization of the central potential is energy dependent, i.e., increasing with projectile energy [22].

A $^6\vec{\text{Li}}$ data set that has small AP errors over a large angular range, and that is complete at two widely spaced energies would help to answer these questions. This work reports new inelastic-scattering AP's for $^6\text{Li}+^{12}\text{C}$ at $E_{\text{lab}}(^6\text{Li})=50$ MeV, which, in combination with the 30 MeV data of Reber *et al.* [10], furnishes two data sets for the same target at incident energies substantially above the Coulomb barrier. In addition, new data are reported for the excitation of states in ^{6}Li at the same c.m. energy (33.3 MeV) by using a 100 MeV ^{12}C beam to bombard a ^{6}Li target.

The present work presents the results of a CC analysis of both data sets. The CC analysis seeks to determine, at both energies, the role of projectile and target-excitation channel coupling and the role of the explicit and dynamic spin-orbit and tensor interactions in generating the different analyzing powers. In this way, the energy dependence of the spin-dependent interactions involved in the scattering is examined.

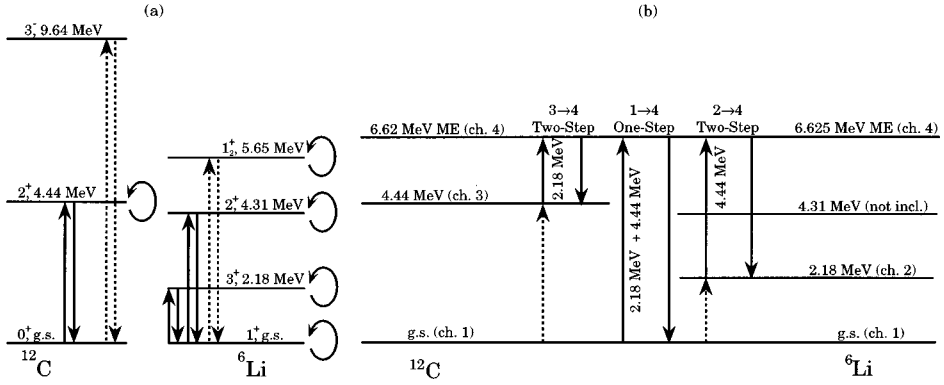

FIG. 1. (a) The four- and six-channel coupling schemes used with the code FRESCO. The solid arrows show the four-channel scheme and the dashed arrows show the additional channels included in the six-channel scheme. (b) The one- and two-step coupling schemes for the ^{6}Li + ^{12}C mutual excitation (ME). The channel numbers assigned to each energy level are given in parentheses.

II. EXPERIMENT

The experimental details of the measurements of inelastic-scattering AP's are the same as given earlier in a report focusing on the elastic scattering [23]. After the measurement of cross sections and AP's for ^{12}C($^{6}\vec{\text{Li}}$, ^{6}Li) at 50 MeV were completed, measurements of cross sections for the inverse-kinematics reaction ^{6}Li(^{12}C, ^{12}C) at 100 MeV were carried out. The motivation for this experiment was to measure the cross sections for the excited states of ^{6}Li. These cross sections are related directly to the strength with which the ^{6}Li* channels couple to the elastic and inelastic ^{12}C* channels, and thus allow the coupling-strength parameters to be fixed in the CC analysis of the 50 MeV ^{12}C($^{6}\vec{\text{Li}}$, ^{6}Li) cross section and AP data.

The ^{6}Li target material (enriched to 99%) was deposited on a Formvar backing and transferred to an 85 cm diameter target chamber under vacuum. This has been found necessary because the humid air present in the laboratory reacts quickly with lithium, which then dissolves on the backing. Even with considerable care, carbon, oxygen, and silicon contaminants were found in the ^{6}Li target. A ^{12}C target that had roughly the same amount of contaminants as found in the ^{6}Li target was used at each angle that was used with the ^{6}Li target. The cross sections were measured at the laboratory angles of 4.5°, 5°, 6°, 7°, 10°, 11°, 12°, and 13°. Spectra for both targets were obtained at each angle before the detectors were moved to the next angle because the kinematic shift in energy of the peaks is quite rapid when inverse kinematics is used.

Once the contaminant peaks are identified in the ^{12}C target spectra at a given angle, they can be accounted for in the ^{6}Li target spectra at the same angle. Other peaks remaining in the ^{6}Li spectra are only from the ^{6}Li(^{12}C, ^{12}C)^{6}Li* reactions, whose yields are used to produce the ^{6}Li* cross sections by normalizing them to the known elastic-scattering cross sections. Cross sections could be obtained in this way for the excited states 3^{+}(2.18 MeV), 2^{+}(4.31 MeV), and 1^{+}(5.65 MeV) of ^{6}Li. Beyond the 5.65 MeV state, there were too many states in the continuum part of the spectrum, making peak identification impossible.

III. ANALYSIS

Both the new 50 MeV and the previously published 30 MeV data on elastic and inelastic ^{6}Li + ^{12}C scattering were analyzed with CC calculations using double-folded (DF) real and Woods-Saxon (WS) imaginary central potentials. The use of a semimicroscopic real interaction reduces the number of parameters in the calculation, allowing the underlying mechanisms that are responsible for producing different analyzing powers to be identified more clearly.

The initial calculations used a version of the CC code CHUCK [24,25] that allows projectile excitation as well as target excitation to be incorporated in the calculations, but can couple together only up to four channels. The calculations with CHUCK were used as a starting point because of similar work done earlier at 30 MeV using this code [8,10]. The starting parameters were taken from the work of Reber *et al.* [10]. Later calculations employed the code FRESCO [26], which allowed more channels to be included. Extensive tests were carried out with FRESCO using an external read-in DF potential to make certain that the calculated analyzing powers gave the same results as the well-tested projectile-excitation version of CHUCK. Other interactions were introduced into the calculations in attempts to improve the agreement with observables that eluded simple description. These included an imaginary SO potential, a deformed SO coupling potential, and ^{6}Li + ^{12}C mutual excitation. The results of these calculations are discussed in subsection B.

A. Calculations

The calculations with the code FRESCO included six channels: the ground state, the first three excited states of ^{6}Li, and the first two nonzero-spin excited states of ^{12}C. The reorientation terms for all channels except the ^{12}C(9.64 MeV) channel, which has a zero quadrupole reorientation Clebsch-Gordan coefficient, were included. The solid arrows in Fig. 1(a) show a four-channel coupling scheme and the dashed arrows show the two additional channels included for the six-channel coupling scheme. The curled arrows represent the reorientation terms.

The real central potential for ^{6}Li + ^{12}C was obtained in the DF formalism [18,27] using the M3Y effective nucleon-nucleon interaction of Bertsch *et al.* [28] (the $S=T=0$ term only), supplemented with a term approximating single-nucleon knockout exchange (SNKE) [29]. The nucleon density of ^{6}Li was obtained from the measured charge density of Suelzle [30] by assuming that the proton and neutron distributions have the same shape. The nuclear density of ^{12}C was obtained from a modified harmonic oscillator density [31]. For strong collective excitations, the radial part of the tran-

sition density is concentrated near the nuclear surface and, to first-order in deformation, is given by the derivative of the nucleon density $\rho(r)$:

$$\rho^{ij}_{\ell}(r) = -\delta^{ij}_{\ell}\frac{d\rho(r)}{dr}. \tag{1}$$

Here, δ^{ij}_{ℓ} is the 2^{ℓ}-pole deformation length for a transition from state i to state j. The deformed densities are then used in the DF formalism to obtain the real central transition potential.

The imaginary central potential was of the Woods-Saxon (WS) form:

$$W_{\text{diagonal}}(r) = \frac{-W_0}{1+\exp\left(\dfrac{r-R_I}{a_I}\right)}. \tag{2}$$

The imaginary central transition potential is obtained by taking the derivative of the imaginary central potential, using the same deformation length δ^{ij}_{ℓ} as in the DF real transition potential:

$$W_{\text{coupling}}(r) = -\delta^{ij}_{\ell}\frac{d}{dr}\frac{-W_0}{1+\exp\left(\dfrac{r-R_I}{a_I}\right)}. \tag{3}$$

Also included was a real spin-orbit interaction of the Thomas form:

$$V_{\text{SO}}(r) = \left(\frac{\hbar}{m_{\pi}c}\right)^2\frac{V_{\text{SO}}}{r}\frac{d}{dr}f_{\text{SO}}(r)\,\vec{l}\cdot\vec{s}, \tag{4}$$

where $\vec{s}$ is the spin operator of the $s=1$ spin of ^{6}Li and

$$f_{\text{SO}}(r) = \left[1+\exp\left(\frac{r-R_{\text{SO}}}{a_{\text{SO}}}\right)\right]^{-1}. \tag{5}$$

The coupling strengths for the excitation of the ^{6}Li(2.18 MeV), ^{6}Li(4.31 MeV), ^{6}Li(5.65 MeV), ^{12}C(4.44 MeV), and ^{12}C(9.64 MeV) states are given by the deformation lengths, denoted as $\delta_2(2.18)$, $\delta_2(4.31)$, $\delta_2(5.65)$, $\delta_2(4.44)$, and $\delta_3(9.64)$, respectively. Alternatively, these strengths can be specified in terms of parameters β_{ℓ} given, for example, by the relation $\delta_{\ell}=\beta_{\ell}R_I=\beta_{\ell}r_I A_T^{1/3}$, where R_I is the full radius of the imaginary central potential and A_T is the target mass number. Coupling strengths were set by matching the calculated inelastic-scattering cross sections to the experimental data. The 50 MeV ^{12}C* cross section data were obtained in the measurement of the AP iT_{11} and supplemented with the data taken by Trcka *et al.* [32]. The ^{6}Li* cross section data are described in Sec. II above. In addition to the transition coupling strengths, there are also the parameters of the reorientation terms for the ^{6}Li(2.18 MeV), ^{6}Li(4.31 MeV), ^{6}Li(5.65 MeV), and ^{12}C(4.44 MeV) excited states, and the ground state (g.s.), denoted as β_2(2.18r), β_2(4.31r), β_2(5.65r), β_2(4.44r), and β_2(g.s.r), respectively. The transition and reorientation coupling strengths used at 30 MeV were the same as those used at 50 MeV.

B. Results

1. Comparison between calculations with the codes FRESCO *and* CHUCK

The initial calculations with the code CHUCK focused on the 50 MeV elastic-scattering cross section as ratio-to-Rutherford (σ/σ_R) and AP iT_{11}, since these data have the smallest errors and since iT_{11} was found in an earlier optical-model analysis to be sensitive to all spin-dependent forces [23]. The calculations were then refined to describe additionally the elastic-scattering AP T_{20}. Then the calculations focused on the 30 MeV data, starting from the 50 MeV parameter set. Finally, the calculations alternated between those for 30 and 50 MeV in order to describe all the data with as few parameter differences as possible. A four-channel coupling scheme, given in Fig. 1(a), was used in these CC calculations.

After the four-channel CHUCK calculations, the goal was to reproduce these results with FRESCO as a check between the CHUCK and FRESCO codes. Beginning with simplified trial runs and working up to the full four-channel calculation, very good agreement between the codes CHUCK and FRESCO was obtained when care was taken in setting the numerical-accuracy parameters. The results of this comparison are given here briefly

(1) Optical model (OM) calculations with the code HERMES [33] using standard Woods-Saxon (WS) forms have been reproduced with FRESCO.

(2) Double-folded real central potential OM calculations of HERMESV (HERMES modified to handle DF real central potentials) have been reproduced with FRESCO by reading in a DF real central potential.

(3) Coupled-channels calculations of the code CHUCK have been reproduced with FRESCO. The couplings included projectile excitation, target excitation, and reorientation. Both WS real central and DF real central potential calculations of CHUCK have been reproduced.

(4) When due regard is taken of the different definitions of the spin orbit-potential strengths (the parameter of the SO potential strength in FRESCO is factors of 1/2 and 1/4 of that in HERMES and CHUCK, respectively), the AP's calculated with all the three codes agree.

(5) A radial integration step size of 0.05 fm was used in FRESCO to reproduce CHUCK calculations with a step size of 0.1 fm.

(6) Three methods of coupling channels in FRESCO were investigated and each agrees with the corresponding CHUCK calculations.

The 50 and 30 MeV four-channel FRESCO parameters are given in Table I as parameter sets A and B, respectively.

2. Combined description of 50 and 30 MeV cross sections and analyzing powers

The ^{6}Li(5.65 MeV) and ^{12}C(9.64 MeV) states were then added to the above four-channel FRESCO calculations. The resulting six-channel calculations describe both the 30 and 50 MeV σ/σ_R and elastic iT_{11} very well with only few differences in the parameters between the two energies. Parameter sets C (50 MeV) and D (30 MeV) in Table I give the six-channel FRESCO parameters for the combined description at both energies. Figure 2 shows the elastic-scattering data

TABLE I. Parameters of the four- and six-channel CC calculations with the code FRESCO. The strength of the FRESCO spin-orbit input parameter is $\frac{1}{4}V_{SO}$ while that for CHUCK is V_{SO}.

			Optical-potential parameters						
Set	N	SNKE (MeV)	W_0 (MeV)	r_I [a] (fm)	a_I (fm)	V_{SO} (MeV)	r_{SO} [a] (fm)	a_{SO} (fm)	
A	0.985	−356.0	12.0	2.22	0.55	2.0	1.8	0.35	Four channels, 50 MeV
B	0.910	−390.0	8.0	2.22	0.55	2.0	1.8	0.8	Four channels, 30 MeV
C	0.985	−356.0	10.0	2.22	0.55	2.0	0.9	0.8	Six channels, 50 MeV
D	0.890	−390.0	7.0	2.22	0.55	2.0	1.8	0.8	Six channels, 30 MeV

				Coupling-strength parameters						
Set	$\beta_2(2.18)$	β_2(g.s.r)	$\beta_2(2.18r)$	$\beta_2(4.31)$	$\beta_2(4.31r)$	$\beta_2(4.44)$	$\beta_2(4.44r)$	$\beta_2(5.65)$	$\beta_2(5.65r)$	$\beta_3(9.64)$
A	−0.4	−0.15	−0.3	−0.3	−0.15	−0.3	−0.15			
B	−0.4	−0.15	−0.3	−0.3	−0.15	−0.3	−0.15			
C	−0.4	−0.15	−0.3	−0.38	−0.19	−0.26	−0.13	−0.73	−0.37	−0.16
D	−0.4	−0.15	−0.3	−0.38	−0.19	−0.26	−0.13	−0.73	−0.37	−0.16

[a] $R_x = r_x 12^{1/3}$.

and calculations at 50 MeV (top) and 30 MeV (bottom). These calculations represent the best six-channel description obtained for the 30 and 50 MeV data. The only differences are in the DF normalization parameters, $N=(0.89,0.985)$, the imaginary WS strengths, $W_0=(7.0,10.0)$ MeV, and SO potential radii, $r_{SO}=(1.8,0.9)$ fm at $E=(30,50)$ MeV.

The elastic-scattering cross section, particularly at 50 MeV, was very sensitive to the DF normalization parameter N, thus $N=0.985$ is chosen over 0.99. The SNKE values were fixed at −390 and −356 MeV, at 30 and 50 MeV, respectively, as given by Stanley [37]. However, it was found that the changes in calculations that were due to changes in the DF parameter N could be compensated for by changing the SNKE value. Therefore, alternatively, N could be fixed and SNKE used as a parameter. This coupling between N and SNKE has been discussed recently by Satchler and Love [38].

In the full calculations, all coupled states had their reorientation included, with strengths that were equal to about the same fraction ($\sim 1/2$) of the state transition strengths. The deformation lengths δ_ℓ^{ij} derived from the β_ℓ parameters used in parameter sets A–D are given in Table II along with values obtained from other references.

The elastic-scattering AP iT_{11} is described very well at both energies. The small-angle rank-2 AP's in the elastic scattering are described reasonably well, except for T_{22}, which is overpredicted at both energies. The most obvious feature that is not described in elastic scattering is the large dip in T_{20} at 50 MeV between 45°–60° c.m. Better descriptions were obtained at both energies, but at the cost of more parameter differences. The parameters of the combined description indicate that the spin-orbit potential is different at 30 and 50 MeV. They also indicate that the DF normalization N approaches unity at the higher energy. This is in agreement with an analysis of $^6\vec{\text{Li}} + {}^{26}\text{Mg}$ scattering at 44 and 60 MeV [6], although deuteron-α cluster-folded (CF) potentials were used in that work. Finally, the strength W of

TABLE II. Deformation lengths for ^{6}Li and ^{12}C.

Nucleus	Transition $(i\to j)$	Q (MeV)	ℓ	Present δ_ℓ^{ij} (fm)	Reber [a] δ_ℓ^{ij} (fm)	$B(E\ell)$ $\lvert\delta_\ell^{ij}\rvert$ (fm) [b]
^{6}Li	$1^+\to 3^+$	−2.18	2	−2.04	−2.04	3.69 [c]
^{6}Li	$1^+\to 1^+$		2	−0.76	−1.02	
^{6}Li	$3^+\to 3^+$		2	−1.53	−1.02	
^{6}Li	$1^+\to 2^+$	−4.31	2	−1.95	−2.04	1.83 [c]
^{6}Li	$2^+\to 2^+$		2	−0.98		
^{6}Li	$1^+\to 1_2^+$	−5.65	2	−3.72		
^{6}Li	$1_2^+\to 1_2^+$		2	−1.86		
^{12}C	$0^+\to 2^+$	−4.44	2	−1.34	−1.35	1.48 [d]
^{12}C	$2^+\to 2^+$		2	−0.67		
^{12}C	$0^+\to 3^-$	−9.64	3	−0.80	−1.29	1.91 [e]

[a] Reference [10].
[b] Deformation lengths determined from $B(E\ell)$ values.
[c] Reference [34].
[d] Reference [35].
[e] Reference [36].

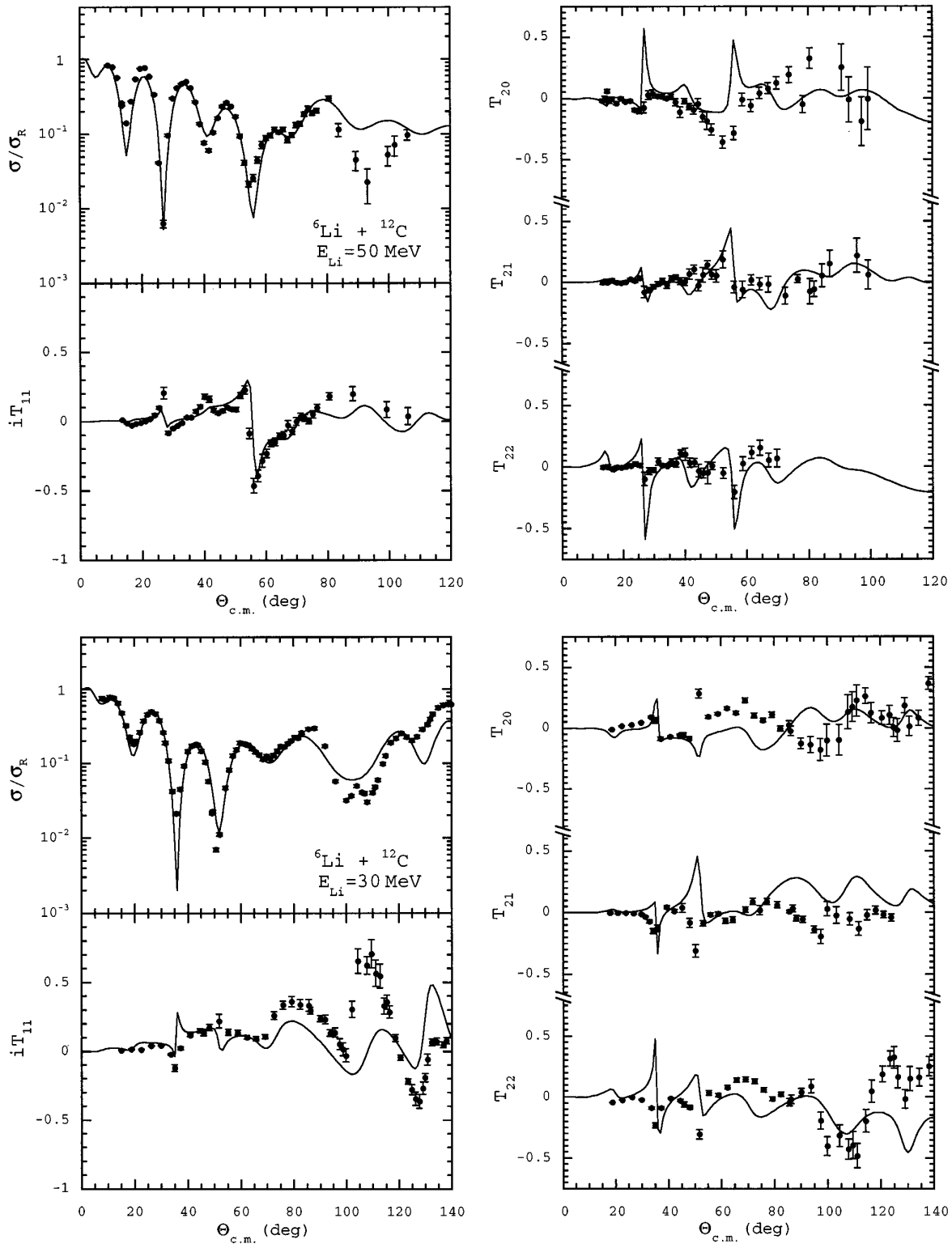

FIG. 2. Six-channel CC calculations for the ^{12}C(^{6}Li,^{6}Li) elastic-scattering cross sections and AP's. The calculation for the energy of 50 MeV (top) uses parameter set C of Table I, and the calculation for 30 MeV (bottom) uses parameter set D of Table I.

the imaginary central potential is greater at 50 MeV, reflecting the fact that, at the higher energy, more reaction channels open up, but are not accounted for explicitly in the calculation.

The ^{12}C(2^+, 4.44 MeV) and ^{12}C(3^-, 9.64 MeV) inelastic-scattering cross sections and AP's were not described nearly as well as the elastic-scattering data. Data for the ^{12}C(0^+, 7.65 MeV) excitation were obtained, but this

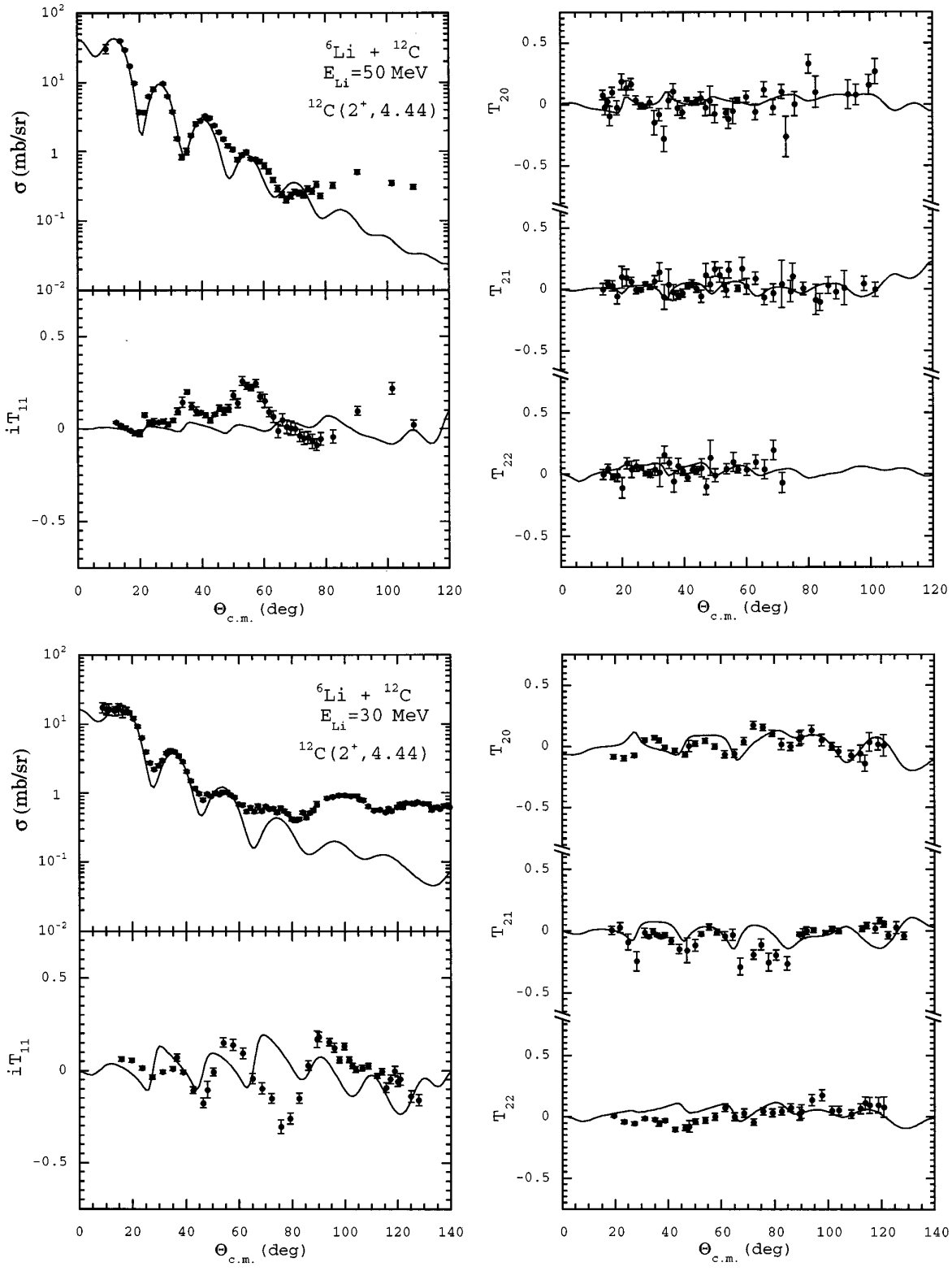

FIG. 3. Six-channel CC calculations for the ^{12}C(4.44 MeV) cross section and AP's. The calculation for the energy of 50 MeV (top) uses parameter set C of Table I, and the calculation for 30 MeV (bottom) uses parameter set D of Table I.

state was not included in the calculations due to the difficulties found with other projectiles in describing this transition. Figure 3 presents the ^{12}C(4.44 MeV) state data and calculations at 50 MeV (top) and 30 MeV (bottom). Figure 4 shows the 50 MeV ^{12}C(7.65 MeV) state data, and Fig. 5 shows the ^{12}C(9.64 MeV) state data and calculations at both energies.

The ^{12}C(4.44 MeV) rank-2 AP's at 50 MeV are small and comparable to the calculations, but there are two well-

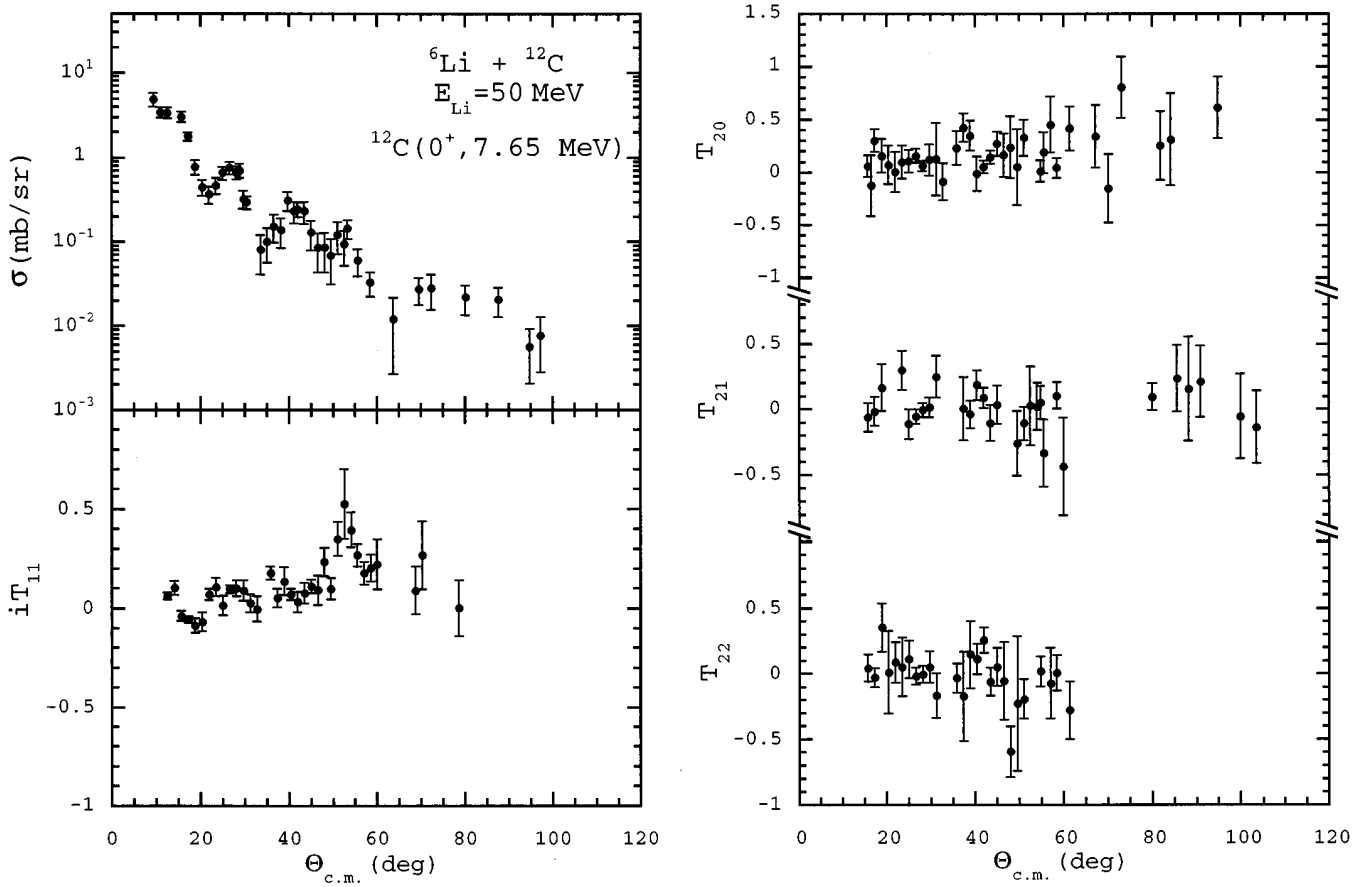

FIG. 4. Experimental data for the ^{12}C(0^{+}, 7.65 MeV) cross section and AP's at 50 MeV.

structured peaks in iT_{11}(4.44 MeV) that were not reproduced in the calculations. In addition, the cross section is underpredicted at large angles. At 30 MeV, the AP calculations match the data in magnitude but not in detail or phase. The calculated ^{12}C(4.44 MeV) cross section is particularly poor beyond 60° c.m., underpredicting markedly the data. In the final description, more weight was placed on the small-angle cross sections and AP's.

At both energies, the ^{12}C(9.64 MeV) experimental AP's are much greater than the calculated values, particularly at 30 MeV. The cross-section calculations are perhaps better for the ^{12}C(9.64 MeV) state than for the ^{12}C(4.44 MeV) state. The exception is a peak in the 30 MeV calculation between 50° and 75° c.m., which is not present in the data.

3. Inelastic-scattering cross sections for the 3^{+}(2.18 MeV), 2^{+}(4.31 MeV), and 1$_2^{+}$(5.65 MeV) states in ^{6}Li

Figure 6 shows the cross section data and calculations for inelastic scattering to the ^{6}Li(2.18 MeV), ^{6}Li(4.31 MeV), and ^{6}Li(5.65 MeV) states at energies corresponding to $E_{\text{lab}}(^{6}\text{Li}) = 50$ MeV (left) and 30 MeV (right) using parameter sets C and D, respectively. The ^{6}Li(2.18 MeV) cross section was very well described at both energies. The ^{6}Li(4.31 MeV) cross-section calculation was adjusted to bring the magnitude close to the average of all the points, but it does not agree with the data in detail. Only 50 MeV ^{6}Li(5.65 MeV) data exist, and the calculation was adjusted to agree with the two data points.

4. Extending the ^{12}C(4.44 MeV) calculations

Additional interactions were investigated in an attempt to improve the agreement between the calculations and data for the 50 MeV ^{12}C(4.44 MeV) cross section and iT_{11}. These were an imaginary SO potential, a deformed SO coupling potential, and couplings to the ^{6}Li(3^{+}) + ^{12}C(2^{+}) mutual-excitation (ME) channel. These three interactions were investigated with the code CHUCK, as it is faster for calculation of one AP. In addition, mutual excitation can be handled currently only in CHUCK.

The imaginary SO potential did affect the calculations, mainly at angles greater than 50° c.m., but did not provide an improvement that would justify its inclusion. The ''Oak-Ridge'' group's deformed SO coupling potential [39] had an effect on the elastic and inelastic-scattering rank-1 AP's, but resulted in no new features or improvement to the calculations. This version of the spin-orbit potential was used by Sherif and Blair [40], and is a limited form of the full deformed Thomas spin orbit.

The ME channel ^{6}Li(2.18 MeV) + ^{12}C(4.44 MeV) was present in the 100 MeV ^{12}C + ^{6}Li data, and its cross section was obtained as described in Sec. II. It was investigated specifically to determine whether a coupling to this channel would improve the ^{12}C(4.44 MeV) state calculations. Two mechanisms of ME were investigated, one-step and two-step excitations. In a one-step excitation, the ground state is coupled directly to the ME channel. A two-step excitation proceeds sequentially, with the projectile (target) excited via

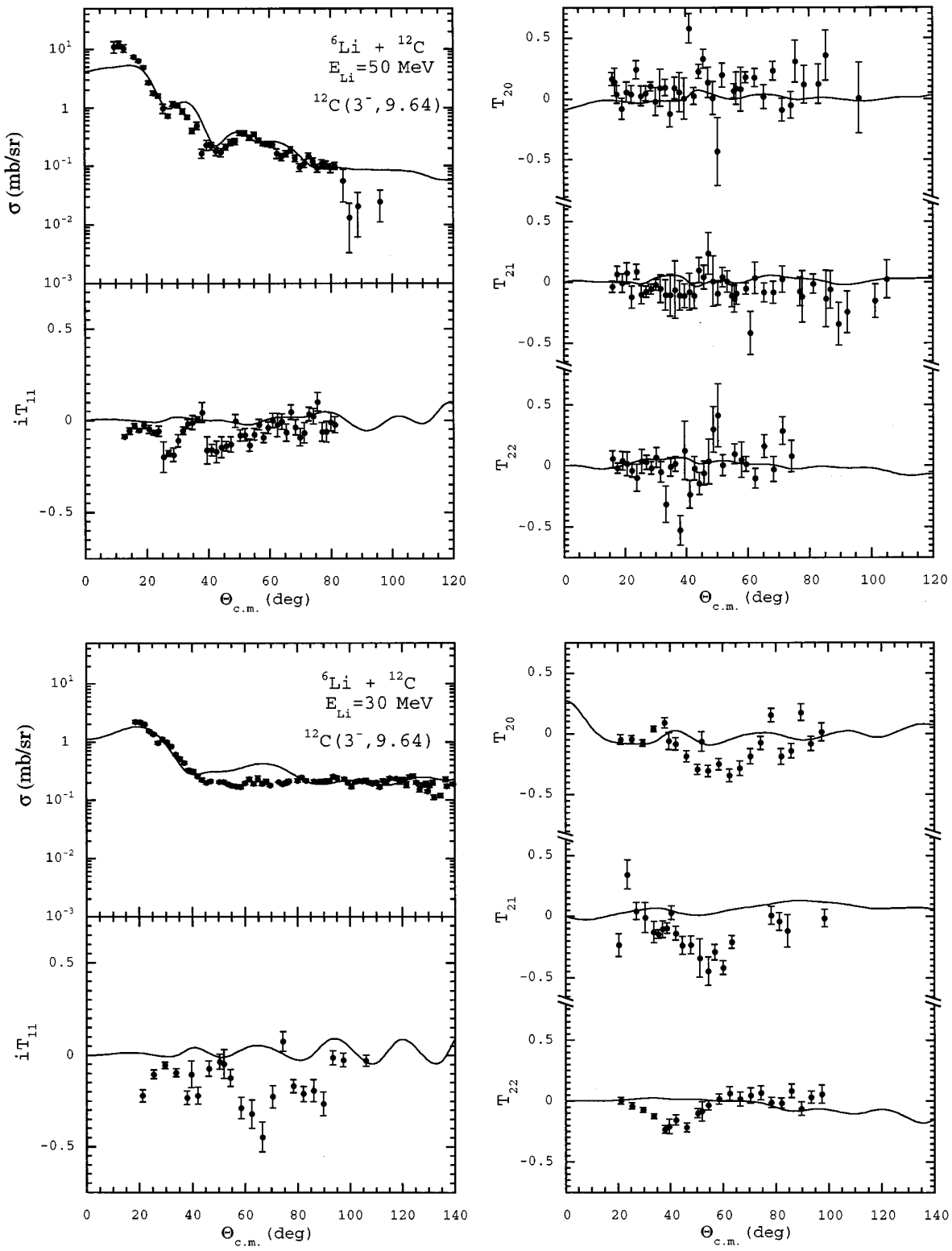

FIG. 5. Six-channel CC calculations for the ^{12}C(9.64 MeV) cross section and AP's. The calculation for the energy of 50 MeV (top) uses parameter set C of Table I, and the calculation for 30 MeV (bottom) uses parameter set D of Table I.

the target (projectile) excited state. In this case, the coupling is between the projectile excited state (target excited state) and the ME channel. Figure 1(b) shows the one-step and two-step ME coupling schemes.

Since the code CHUCK allows for only up to four channels, one of the channels included in previous calculations with CHUCK had to be removed in order to include the 2.18 +4.44 MeV=6.62 MeV ME state. The channel removed was

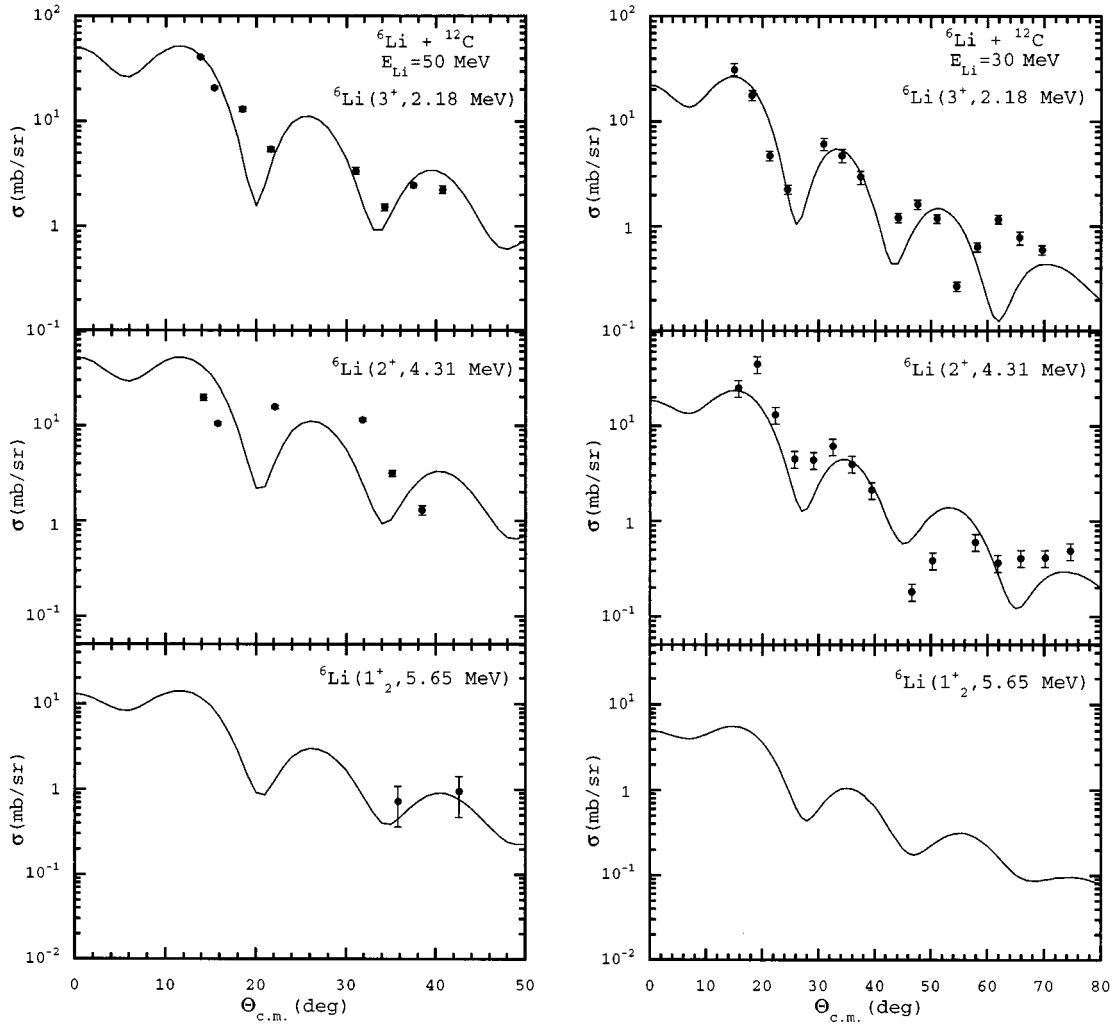

FIG. 6. Six-channel CC calculations for the ^{6}Li(2.18 MeV), ^{6}Li(4.31 MeV), and ^{6}Li(5.65 MeV) cross sections. The calculation for the energy of 50 MeV (left) uses parameter set C of Table I, and the calculation for 30 MeV (right) uses parameter set D of Table I.

the ^{6}Li(4.31 MeV) state, since it had the least important influence in the four-channel calculations. The coupling strength of the one-step ME is proportional to the product of the strengths for the two excited states, and its coupling potential is obtained using a second derivative of the diagonal WS potential for the imaginary part, and both the projectile and target nucleon-density derivatives for the DF real part [41].

The one-step ME can occur with more than one value for the total transferred angular momentum ℓ_{tr}, which is determined vectorially by $\vec{\ell}_{tr}=\vec{s}_{tr}+\vec{j}_{tr}$, with s_{tr} the angular momentum transferred to the projectile and j_{tr} the angular momentum transferred to the target. Since the transfer $s_{tr}=2$ is used for the ^{6}Li(2.18 MeV) state excitation, and the ^{12}C(4.44 MeV) state excitation has $j_{tr}=2$, the one-step ME can occur with a total transferred angular momentum of $\ell_{tr}=0$, 2, or 4. The effect of each of these possibilities was investigated individually and in combination, and found to make no dramatic changes to the calculations. The one-step ME with $\ell_{tr}=4$ contributed most significantly to the ME cross section. It was found that the two-step ME affected all observables, but did not change the general features of the ^{12}C(4.44 MeV) cross section or iT_{11}. The ^{12}C(4.44 MeV) cross section was virtually unchanged. The two-step ME coupling via the ^{12}C(4.44 MeV) state, $1\rightarrow3\rightarrow4$ [see Fig. 1(b)], was the dominant two-step coupling, while the coupling via the ^{6}Li(2.18 MeV) state, $1\rightarrow2\rightarrow4$, had almost no effect. In short, the ^{12}C(4.44 MeV) state data are not described well by the DF CC calculations.

Some other data exist for AP's of excited target states in ^{6}Li scattering. Reber *et al.* [11] obtained data for the $^6\vec{\text{Li}}$ + ^{9}Be*(5/2$^-$, 2.43 MeV) inelastic scattering at 32 MeV. The inelastic-scattering cross section was described well, but the AP iT_{11}(2.43 MeV) was reproduced poorly and had a magnitude similar to the data only when an explicit SO potential was included. Rusek *et al.* [5,6] obtained data for $^6\vec{\text{Li}}+\ ^{26}$Mg*(2$^+$, 1.81 MeV) at 44 and 60 MeV. The 44 MeV inelastic-scattering cross section was described well up to 80° c.m., but, as in the present case, the measured AP iT_{11}(1.81 MeV) is positive while the calculated AP oscillated around zero. The calculated structure is due to the inclusion of a cluster-folded (CF) SO potential. The 60 MeV inelastic-scattering cross section was overpredicted at angles beyond 40° c.m., while the measured AP iT_{11}(1.81 MeV) is small, with calculations in agreement. There are also $^6\vec{\text{Li}}$

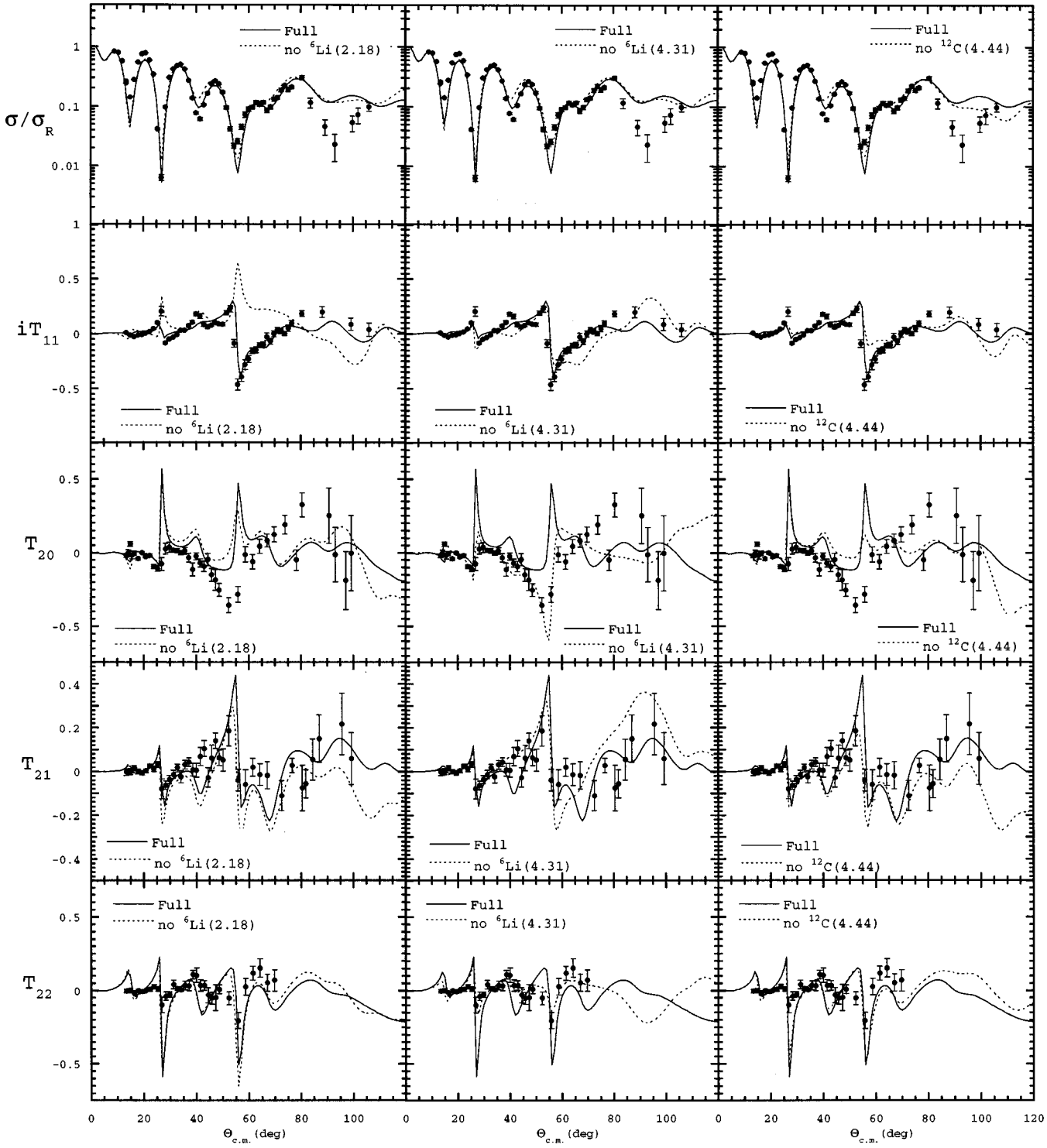

FIG. 7. Six-channel CC calculations for the elastic-scattering cross section and AP's at 50 MeV using parameter set C (solid), and the ^{6}Li(2.18 MeV), ^{6}Li(4.31 MeV), and ^{12}C(4.44 MeV) channel couplings removed one at a time (dashed).

$+^{120}$Sn$^{*}(2^{+}$, 1.1-MeV) data at 44 MeV [14]. The inelastic-scattering cross section and iT_{11}(1.1 MeV) data were described well in calculations which included a CF SO potential and g.s. reorientation.

In each of these cases, the elastic-scattering cross section and AP iT_{11} are accounted for well. The features common to all these inelastic-scattering data sets are that an explicit SO potential is important for the first excited state of the target and that the description of this state worsens at greater projectile energies.

5. Channel coupling and spin-dependent interactions

In order to see their effect on the calculations, each of the five excited-state channel couplings as well as the reorientation terms and SO potential were removed one at a time, and

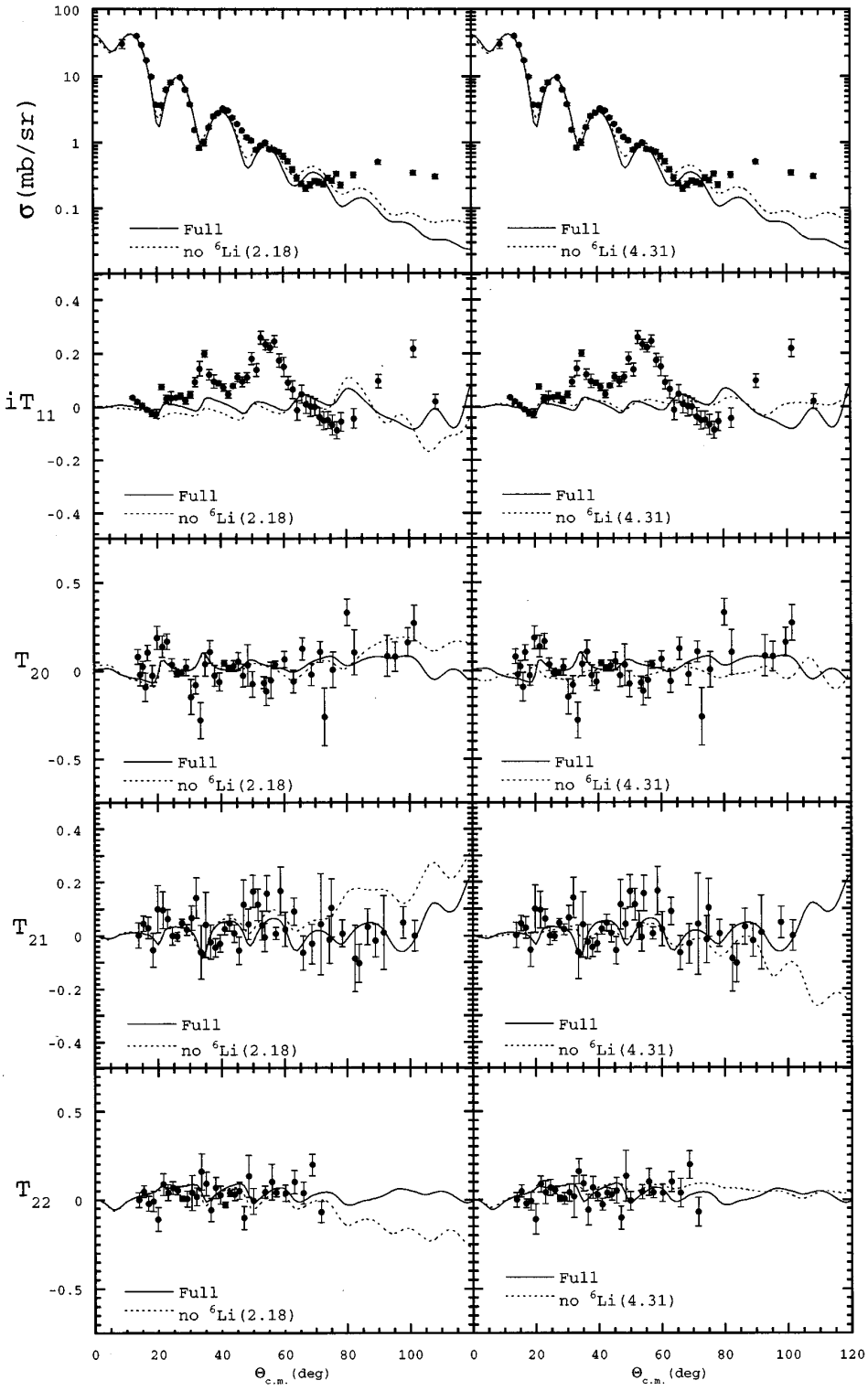

FIG. 8. Six-channel CC calculation of the ^{12}C(4.44 MeV) cross section and AP's at 50 MeV using parameter set C (solid), and the ^{6}Li(2.18 MeV) and ^{6}Li(4.31 MeV) channel couplings removed one at a time (dashed).

compared with the full calculation. With the exception of the g.s. reorientation, the reorientation terms affect the observables in a relatively minor way. The ^{6}Li(5.65 MeV) and ^{12}C(9.64 MeV) state couplings also have relatively minor effects on the measured observables, and so are not included in the comparison. Figure 7 shows the 50 MeV elastic-scattering cross section and AP's with the full calculation of set C (solid), and calculations with each of the ^{6}Li(2.18 MeV), ^{6}Li(4.31 MeV), and ^{12}C(4.44 MeV) states removed separately (dashed). The ^{6}Li(2.18 MeV) coupling has a significant effect on iT_{11} while the ^{6}Li(4.31 MeV) coupling influences significantly T_{20}. Interestingly, the effect of the

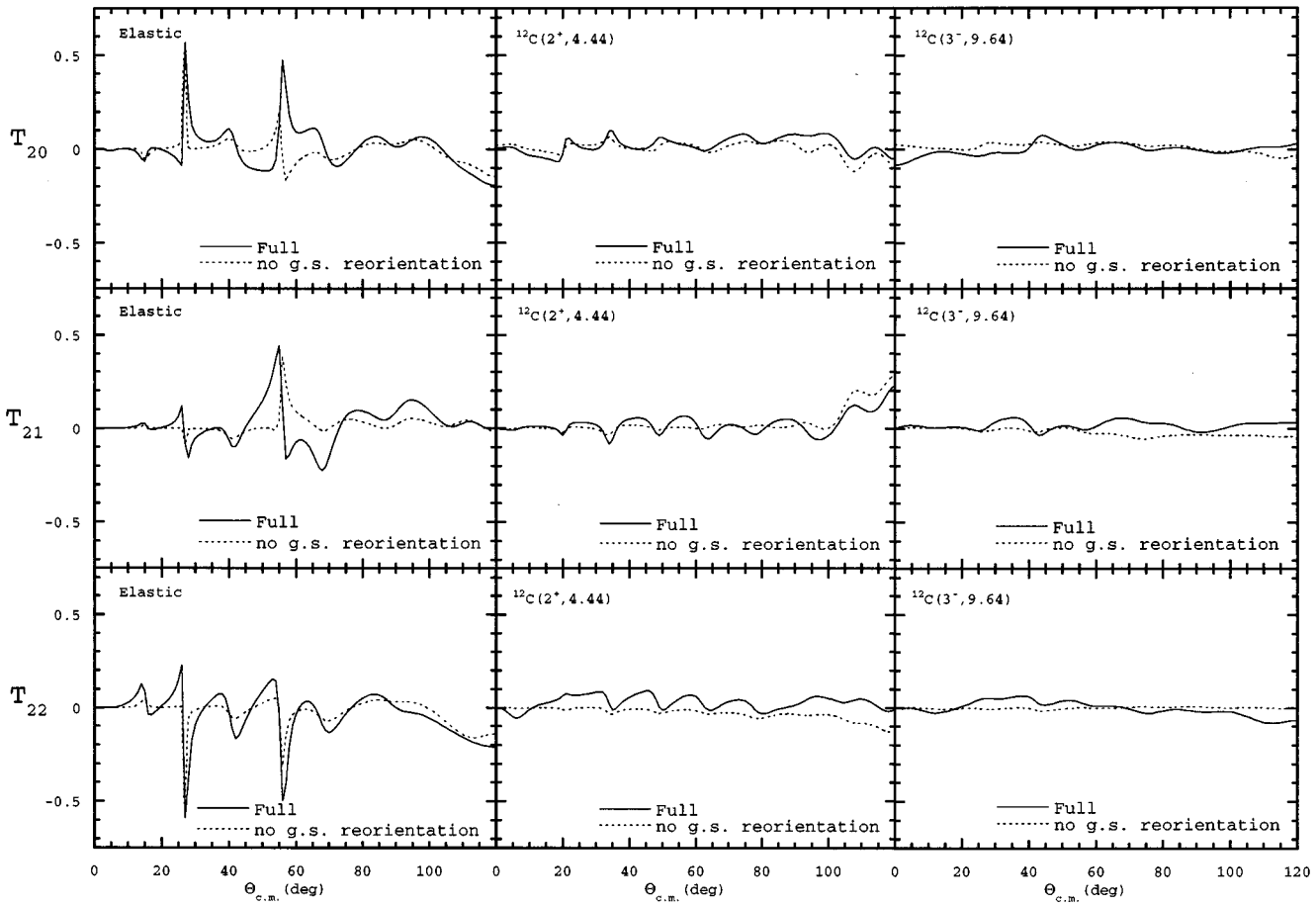

FIG. 9. Six-channel CC calculations for the elastic, ^{12}C(4.44 MeV), and ^{12}C(9.64 MeV) state scattering rank-2 AP's at 50 MeV using parameter set C (solid), and a calculation without the g.s. reorientation (dashed). The data have been left off for clarity.

target excitation ^{12}C(4.44 MeV) is not negligible. Similar results are seen at 30 MeV, except the effect of the ^{6}Li(2.18 MeV) coupling on iT_{11} is reduced somewhat, especially at small angles.

The most dramatic improvement to the description of the data over the optical-model (OM) calculations [23] was for the small-angle region of the elastic-scattering AP iT_{11} at 50 MeV. The present calculations indicate that channel coupling is important for this angular region of iT_{11}, and that the importance of the included channels is greater at 50 MeV than at 30 MeV. This is contrary to the expectation, since a greater projectile energy opens higher-energy reaction channels in the system, and therefore should reduce the importance of any given channel included in CC calculations. However, the persistence of the importance of projectile excitation as projectile energy increases has been observed also with the targets ^{26}Mg [6] and ^{58}Ni [21].

The effects of the ^{6}Li(2.18 MeV) and ^{6}Li(4.31 MeV) couplings on the ^{12}C(4.44 MeV) state cross section and AP's at 50 MeV are shown in Fig. 8. The ^{6}Li(2.18 MeV) coupling influences mainly the rank-2 AP's, and mainly at large angles. The ^{6}Li(4.31 MeV) coupling is important for T_{20} throughout the angular range, while affecting T_{21} and T_{22} mainly at large angles. The ^{6}Li(4.31 MeV) coupling is of less importance for iT_{11} than the ^{6}Li(2.18 MeV) coupling. Similar conclusions hold for the 30 MeV calculations.

The g.s. reorientation has almost no effect on both the cross section and the AP iT_{11} for the elastic scattering and for the excited states ^{12}C(4.44 MeV) and ^{12}C(9.64 MeV) at 30 and 50 MeV. However, this coupling was important for all the rank-2 AP's at 30 and 50 MeV. Reorientation is known to give rise to tensor like interactions [5]. Figure 9 shows the 50 MeV rank-2 full calculations (solid) for the elastic scattering and for the excited states ^{12}C(4.44 MeV) and ^{12}C(9.64 MeV), together with a calculation without the g.s. reorientation term (dashed).

In previous OM calculations [23], a tensor force was needed to produce any sizable elastic-scattering AP T_{21}. In the present CC calculations, the elastic rank-2 AP's are accounted for reasonably well by a dynamic tensor interaction from channel coupling and, therefore, there appears to be no need for an explicit tensor potential in the ^{6}Li-nucleus interaction.

The sensitivity of the elastic-scattering rank-2 AP's to the g.s. reorientation confirms the findings in works on $^6\vec{\text{Li}}$ + ^{26}Mg at 44 MeV [5], $^6\vec{\text{Li}}$ + ^{120}Sn at 44 MeV [14], and $^6\vec{\text{Li}}$ + ^{58}Ni at 70.5 MeV [4,21]. Becker [14] found also that rank-2 AP's for the ^{120}Sn(2$^+$, 1.11 MeV) first excited state were sensitive to this term.

Calculations with the SO potential removed were performed also. The rank-2 AP's were virtually unaffected, but

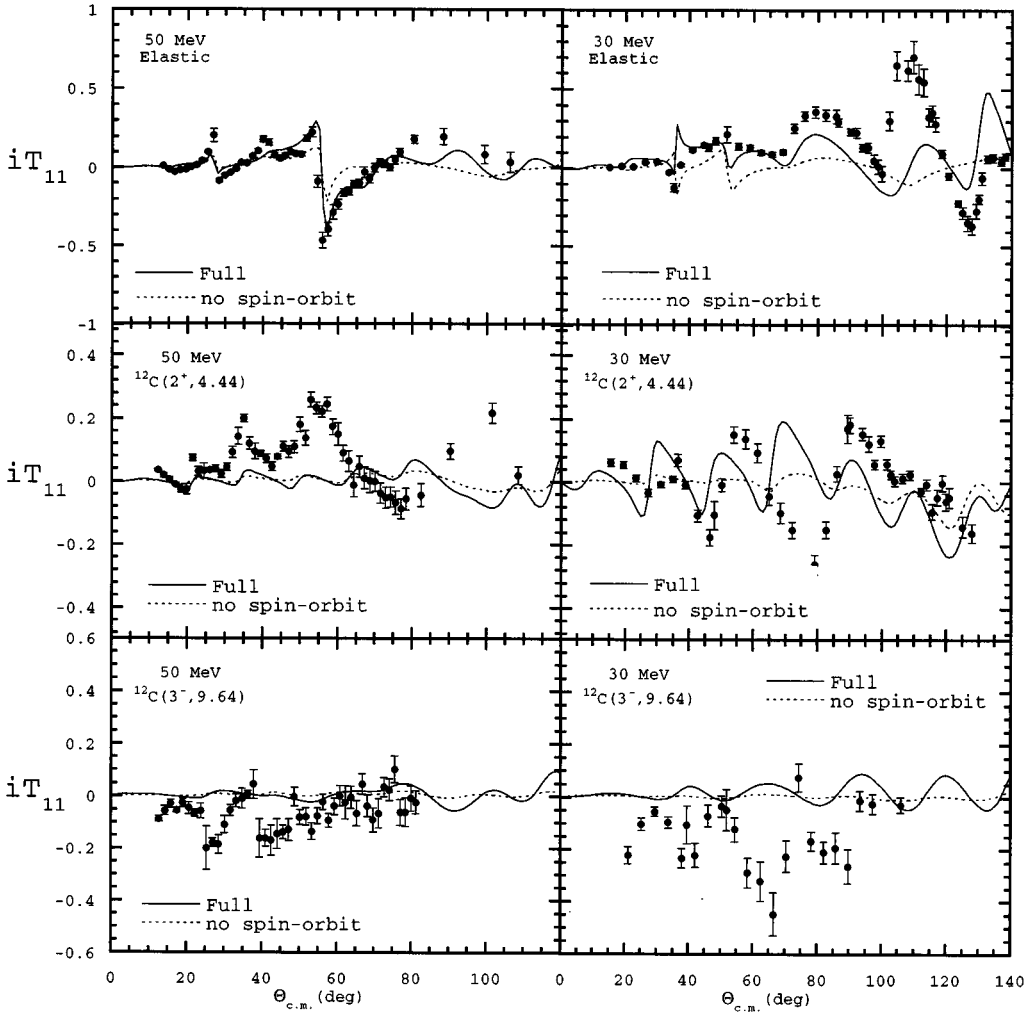

FIG. 10. Six-channel CC calculations for the elastic, ^{12}C(4.44 MeV), and ^{12}C(9.64 MeV) state scattering rank-2 AP's at 50 MeV using parameter set C (solid), and a calculation without the explicit spin-orbit potential (dashed).

the AP's iT_{11} at both 30 and 50 MeV were influenced. Figure 10 shows the full calculations (solid) and the calculations with the SO potential removed (dashed) at 50 MeV (left) and 30 MeV (right). The 30 MeV elastic scattering and inelastic scattering to the ^{12}C(4.44 MeV) and ^{12}C(9.64 MeV) states are very sensitive to the SO potential over the whole angular range. At 50 MeV, the effect is much less pronounced and confined to large angles, except for the elastic-scattering AP iT_{11}, which shows significant deviation from the full calculation around the large inflection at 55° c.m. These calculations indicate that the explicit SO potential is needed to reproduce the data. This is true in particular for the 30 and 50 MeV elastic-scattering AP's iT_{11}, and the 30 MeV inelastic-scattering AP's iT_{11}. Figures 7 and 10 indicate that the small-angle iT_{11}(g.s.) arises mainly from channel coupling at 50 MeV, and from both the channel coupling and an explicit SO potential at 30 MeV.

It is interesting to note the findings of other $^6\vec{\text{Li}}$ work concerning the explicit SO potential. Analyses of $^6\vec{\text{Li}}$ $+\ ^{26}$Mg data at 44 MeV [5,19] showed that the SO potential contributed noticeably to the AP iT_{11}(g.s.), although the dynamic SO interaction dominated. A SO potential for the same reaction at 60 MeV [6] had a more minor effect. An analysis of 44 MeV $^6\vec{\text{Li}}$ + ^{120}Sn scattering [14] drew conclusions similar to those for the 44 MeV ^{26}Mg data. An analysis of $^6\vec{\text{Li}}$ + ^{9}Be data at 32 MeV [11] showed that the SO potential is not so important for the g.s. observables, but very important for the ^{9}Be($5/2^-$, 2.43 MeV) state. Analyses of $^6\vec{\text{Li}}$ + ^{58}Ni scattering at 14.3–22.1 MeV [16] and at 70.5 MeV [4,21] indicate minor roles for the explicit SO potential. On the other hand, analyses of $^6\vec{\text{Li}}$ + ^{4}He data at 6–9.1 MeV c.m. [12,16,42,43] and at 27.9 MeV c.m. [13] point to a significant role for an explicit SO potential.

IV. CONCLUSIONS

A complete set of analyzing powers, iT_{11}, T_{20}, T_{21}, and T_{22}, has been measured for elastic scattering and inelastic scattering to the excited states ^{12}C(2^+, 4.44 MeV), ^{12}C(0^+, 7.65 MeV), and ^{12}C(3^-, 9.64 MeV) in the system $^6\vec{\text{Li}}+\ ^{12}$C at a ^{6}Li beam energy of 50 MeV. This is the highest-energy complete set of AP's measured for $^6\vec{\text{Li}}$, and it contains the highest-energy AP T_{21} measured so far. Com-

bining these data with the 30 MeV data of Reber *et al.* [10] provides the only two complete sets of $^6\vec{\text{Li}}$-scattering data for the same target at energies substantially above the Coulomb barrier.

A coupled-channels analysis of these two sets of data has been carried out with the codes CHUCK and FRESCO, using DF real central potentials. A direct comparison has been made between the two codes, and four-channel CHUCK calculations have been reproduced very well with FRESCO.

The ^{6}Li coupling strengths in the CC calculations were set to reproduce the magnitudes of the cross sections for the excited states of ^{6}Li, which were obtained using the inverse kinematics reaction $^6\text{Li}(^{12}\text{C},^{12}\text{C})^6\text{Li}^*$ at $E_{\text{lab}}(^{12}\text{C})=100$ MeV. The c.m. energy of the $^{12}\text{C}+{}^6\text{Li}$ system is the highest ever used in $^6\text{Li}^*$ cross section measurements.

The present analysis employed six-channel CC calculations, which included the first three excited states of ^{6}Li and the first two nonzero-spin excited states of ^{12}C, and DF real central potentials. Very good descriptions of the 30 and 50 MeV $^{12}\text{C}(^6\vec{\text{Li}},^6\text{Li})^{12}\text{C}$ elastic-scattering cross sections and AP's were obtained. However, the inelastic-scattering cross sections, $^{12}\text{C}(3^-)$ AP's, and $^{12}\text{C}(2^+)$ AP iT_{11} are described poorly. The four-channel calculations provided just as good a description of the data as the six-channel calculations.

At both energies, projectile excitation is very important for the details of the elastic and inelastic-scattering AP's, but not so for the cross sections. The ^{6}Li(2.18 MeV) state has an especially strong effect on the elastic-scattering AP iT_{11} at 50 MeV, and the ^{6}Li(4.31 MeV) state has a particularly strong effect, comparable to the g.s. reorientation, on the rank-2 elastic and inelastic-scattering AP's. The target excitation $^{12}\text{C}(2^+$, 4.44 MeV) is also important, affecting strongly all cross sections and AP's, except those for the ^{12}C(9.64 MeV) state, at both energies. The ^{12}C(9.64 MeV) coupling had an influence on the large-angle cross sections, but had almost no effect on the AP's. The ^{6}Li(5.65 MeV) coupling had some effect on the magnitude of the elastic-scattering AP's.

The imaginary SO and $^6\text{Li}+{}^{12}\text{C}$ mutual-excitation terms provided no noticeable improvement to the description of the elastic and inelastic-scattering data. A deformed SO coupling potential was also investigated. It led to no new features or improvement in the calculations that would justify its inclusion.

The effect of the g.s. reorientation term was found to be very significant for the elastic and inelastic-scattering rank-2 AP's at 30 and 50 MeV. An explicit tensor force was not needed for a reasonable description of the elastic-scattering rank-2 AP's. This indicates that the tensor interaction required to describe the elastic-scattering rank-2 AP's is due mainly to channel coupling effects. Other reorientation terms had only a relatively minor influence on the observables.

Calculations in which the explicit SO potential was removed indicate that, while the explicit SO effects are smaller than the dynamical SO effects, they are significant nevertheless. The explicit SO potential is more important for the inelastic-scattering AP's iT_{11} than for the elastic-scattering iT_{11}, and is much less important at 50 MeV than at 30 MeV. This does not contradict the prediction of Sakuragi [20], but does indicate that the effect of the explicit SO potential does not increase steadily over CC effects as the projectile energy increases.

It has been suggested that the DF normalization is energy dependent, increasing with projectile energy, and that for bombarding energies greater than 10 MeV/nucleon, analyses of $^6\vec{\text{Li}}$ scattering would be free of any renormalization [22]. The present results support this suggestion: the DF normalization $N=0.91$ at 5.0 MeV/nucleon (incident ^{6}Li energy 30 MeV), and $N=0.985$ at 8.3 MeV/nucleon (incident ^{6}Li energy 50 MeV).

ACKNOWLEDGMENTS

The authors wish to acknowledge informative discussions with Dr. R. C. Johnson, Dr. F. Petrovich, Dr. D. Robson, Dr. K. Rusek, Dr. I. J. Thompson, and Dr. J. A. Tostevin. This work was supported by the National Science Foundation and the State of Florida.

[1] W. Weiss, P. Egelhof, K. D. Hildenbrand, D. Kassen, M. Makowska-Rzeszutko, D. Fick, H. Ebinghaus, E. Steffens, A. Amakawa, and K.-I. Kubo, Phys. Lett. **61B**, 237 (1976).

[2] K. Rusek, Z. Moroz, R.Čaplar, P. Egelhof, K.-H. Möbius, E. Steffens, I. Koenig, D. Weller, and D. Fick, Nucl. Phys. **A407**, 208 (1983).

[3] R. P. Ward, N. M. Clarke, K. I. Pearce, C. N. Pinder, C. O. Blyth, H. D. Choi, P. R. Dee, S. Roman, G. Tungate, and N. J. Davis, Phys. Rev. C **50**, 918 (1994).

[4] P. R. Dee, C. O. Blyth, H. D. Choi, N. M. Clarke, S. J. Hall, O. Karban, I. Martel-Bravo, S. Roman, G. Tungate, R. P. Ward, N. J. Davis, D. B. Steski, K. A. Connell, and K. Rusek, Phys. Rev C **51**, 1536 (1995).

[5] K. Rusek, J. Giroux, H. J. Jänsch, H. Vogt, K. Becker, K. Blatt, A. Gerlach, W. Korsch, H. Leucker, W. Luck, H. Reich, H.-G. Völk, and D. Fick, Nucl. Phys. **A503**, 223 (1989).

[6] K. Rusek, N. M. Clarke, and R. P. Ward, Phys. Rev. C **50**, 2010 (1994).

[7] M. Makowska-Rzeszutko, P. Egelhof, D. Kassen, E. Steffens, W. Weiss, D. Fick, W. Dreves, K.-I. Kubo, and T. Suzuki, Phys. Lett. **74B**, 187 (1978).

[8] S. P. Van Verst, D. P. Sanderson, D. E. Trcka, K. W. Kemper, V. Hnizdo, B. G. Schmidt, and K. R. Chapman, Phys. Rev. C **39**, 853 (1989).

[9] E. L. Reber, K. W. Kemper, P. L. Kerr, A. J. Mendez, E. G. Myers, and B. G. Schmidt, Phys. Rev. C **49**, R1 (1994).

[10] E. L. Reber, K. W. Kemper, P. V. Green, P. L. Kerr, A. J. Mendez, E. G. Myers, B. G. Schmidt, and V. Hnizdo, Phys. Rev. C **50**, 2917 (1994).

[11] E. L. Reber, K. W. Kemper, P. L. Kerr, A. J. Mendez, E. G. Myers, B. G. Schmidt, and V. Hnizdo, Phys. Rev. C **48**, 285 (1993).

[12] P. Egelhof, J. Barrelle, P. Braun-Munzinger, W. Dreves, C. K. Gelbke, D. Kassen, E. Steffens, W. Weiss, and D. Fick, Phys. Lett. **84B**, 176 (1979).
[13] P. V. Green, K. W. Kemper, P. L. Kerr, K. Mohajeri, E. G. Myers, D. Robson, K. Rusek, and I. J. Thompson, Phys. Rev. C **53**, 2862 (1996).
[14] K. Becker, K. Blatt, H. J. Jänsch, W. Korsch, H. Leucker, W. Luck, H. Reich, H.-G. Völk, D. Fick, and K. Rusek, Nucl. Phys. **A535**, 189 (1991).
[15] H. Nishioka, R. C. Johnson, J. A. Tostevin, and K.-I. Kubo, Phys. Rev. Lett. **48**, 1795 (1982).
[16] H. Nishioka, J. A. Tostevin, R. C. Johnson, and K.-I. Kubo, Nucl. Phys. **A415**, 230 (1984).
[17] H. Ohnishi, M. Tanifuji, M. Kamimura, Y. Sakuragi, and M. Yahiro, Nucl. Phys. **A415**, 271 (1984).
[18] F. Petrovich, R. J. Philpott, A. W. Carpenter, and J. A. Carr, Nucl. Phys. **A425**, 609 (1984).
[19] Y. Hirabayashi and Y. Sakuragi, Nucl. Phys. **A536**, 375 (1992).
[20] Y. Sakuragi, Phys. Lett. B **220**, 22 (1989).
[21] K. Rusek, N. M. Clarke, G. Tungate, and R. P. Ward, Phys. Rev. C **52**, 2614 (1995).
[22] Y. Hirabayashi, Phys. Lett. B **258**, 11 (1991).
[23] P. L. Kerr, K. W. Kemper, P. V. Green, K. Mohajeri, E. G. Myers, D. Robson, and B. G. Schmidt, Phys. Rev. C **51**, 1924 (1995).
[24] P. D. Kunz, University of Colorado (unpublished).
[25] V. Hnizdo (unpublished).
[26] I. J. Thompson, Comput. Phys. Rep. **7**, 167 (1988).
[27] G. R. Satchler and W. G. Love, Phys. Rep. **55**, 183 (1979).
[28] G. Bertsch, J. Borysowicz, H. McManus, and W. G. Love, Nucl. Phys. **A284**, 399 (1977).
[29] M. Golin, F. Petrovich, and D. Robson, Phys. Lett. **64B**, 253 (1976).
[30] L. R. Suelzle, M. Y. Yearian, and H. Crannell, Phys. Rev. **162**, 992 (1967).
[31] W. D. Myers, Nucl. Phys. **A145**, 387 (1970).
[32] D. E. Trcka, A. D. Frawley, K. W. Kemper, D. Robson, J. D. Fox, and E. G. Myers, Phys. Rev. C **41**, 2134 (1990).
[33] J. Cook, Comput. Phys. Commun. **31**, 363 (1984).
[34] F. Eigenbrod, Z. Phys. **228**, 337 (1969).
[35] P. H. Stelson and L. Grodzins, Nucl. Data Tables **1A**, 21 (1965).
[36] H. Crannell, Phys. Rev. **148**, 1107 (1966); P. Strehl and T. H. Schucan, Phys. Lett. **27B**, 641 (1968); H. Crannell, J. T. O'Brien, and D. I. Sober, in *Proceedings of International Conference on Nuclear Physics with Electromagnetic Interactions*, Mainz, 1979, edited by H. Arenhovel and D. Drechsel (Springer, Berlin, 1979).
[37] D. Stanley, Ph.D. thesis, Florida State University, 1979.
[38] G. R. Satchler and W. G. Love, Phys. Rev. C **49**, 2254 (1994).
[39] M. P. Fricke, R. M. Drisko, R. H. Bassel, E. E. Gross, B. J. Morton, and A. Zucker, Phys. Rev. Lett. **16**, 746 (1966).
[40] H. Sherif and J. Blair, Phys. Lett. **26B**, 489 (1968).
[41] V. Hnizdo and K.W. Kemper, Phys. Rev. C **38**, 1242 (1988).
[42] H. R. Blieden, G. M. Temmer, and K. L. Warsh, Nucl. Phys. **49**, 209 (1963).
[43] H. G. Bingham, K. W. Kemper, and N. R. Fletcher, Nucl. Phys. **A175**, 374 (1971).